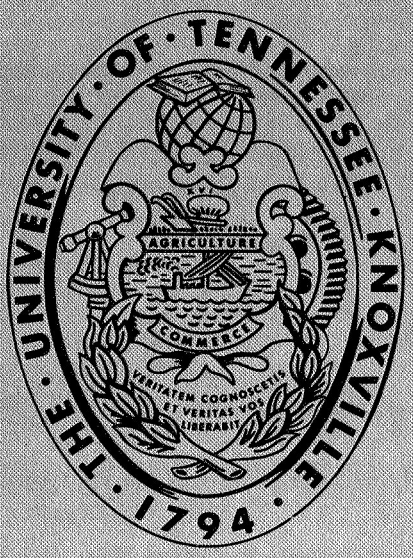

ELECTRIC FIELD INDUCED PURE ROTATION SPECTRUM OF HYDROGEN

William Joseph Boyd III

May 1969

Work performed under N.A.S.A. Grants
~~NsG-539~~ and NGL 43-001-006

THE UNIVERSITY OF TENNESSEE
Knoxville, Tennessee

May 22, 1969

To the Graduate Council:

I am submitting herewith a thesis written by William Joseph Boyd, III, entitled "Electric Field Induced Pure Rotation Spectrum of Hydrogen." I recommend that it be accepted for nine quarter hours of credit in partial fulfillment of the requirements for the degree of Master of Science, with a major in Physics.

_____
Major Professor

We have read this thesis
and recommend its acceptance:

_____

_____

Accepted for the Council:

_____
Vice Chancellor for
Graduate Studies and Research

ELECTRIC FIELD INDUCED PURE ROTATION SPECTRUM OF HYDROGEN

A Thesis

Presented to

the Graduate Council of

The University of Tennessee

In Partial Fulfillment

of the Requirements for the Degree

Master of Science

by

William Joseph Boyd, III

June 1969

ACKNOWLEDGMENTS

The author wishes to acknowledge Dr. N. M. Gailar for his personal supervision, and for making funds available for the experiment. Thanks is extended to Dr. W. E. Blass for help in the analysis of the data. Also acknowledgment is given to Mr. Ray Mink of the Instrument Shop and Mr. Glen Cunningham of the Electronics Shop of the Physics Department at The University of Tennessee for their work and suggestions.

The author gratefully acknowledges the personal help and direction of Dr. P. J. Brannon, whose experience in the field of electric field induced spectrum and many suggestions, made the improved cell possible.

A special acknowledgment is given to the author's parents for their encouragement and financial assistance throughout the years of study.

The financial aid given by the National Aeronautics and Space Administration under Research Grant NSG-539 and Research Grant NGL 43-001-006 was sincerely appreciated.

ABSTRACT

A new Stark cell capable of producing higher electric field intensities than had been before achieved was built and used to examine the pure rotation infrared spectrum of the hydrogen molecule. The higher field intensities were achieved by the elimination of plastic spacers traditionally used in previous Stark cells between the parallel plate electrodes. Operating field intensities of 200,000 volts/cm. are easily obtained in compressed hydrogen at a pressure of 400 p.s.i., compared to a previous maximum of 135,000 volts/cm. at 550 p.s.i. in a similar cell. Peak field intensity in the new cell just before breakdown is 240,000 volts/cm. in hydrogen at 400 p.s.i.

The fundamental vibration-rotation spectrum and the pure rotation spectrum of hydrogen were observed using the new cell. The pure rotation spectrum was measured since it has not been observed before using the electric field induced method. The frequencies of the $S_o(1)$, $S_o(2)$ and $S_o(3)$ transitions were measured to be 587.079 cm^{-1}, 814.523 cm^{-1}, 1034.765 cm^{-1} respectively. These frequencies were used to calculate the molecular constants of hydrogen. The calculated value for B_o was 59.332, for D_o: .0450 and for H_o: 3.1×10^{-5}.

The design of the new cell is described along with the "aging" and cleaning processes necessary for maximum field intensities. The design and operational performance of a carbon rod furnace built

for use as an infrared source is presented in detail. This furnace operates at a temperature of about $2,600^{\circ}$ Kelvin. Various experimental difficulties as well as changes made in the vacuum spectrometer are discussed.

TABLE OF CONTENTS

LIST OF TABLES

LIST OF FIGURES

CHAPTER I

INTRODUCTION

Homonuclear diatomic molecules such as hydrogen do not ordinarily give rise to an infrared absorption spectrum, since due to symmetry such molecules do not have a permanent or time varying electric dipole moment through which transitions can occur. Transitions can take place, however through the electric quadrupole moment since this moment in non-zero. The intensity of the quadrupolar transitions is about 10^{-6} times that of electric dipole radiation, and the observation of quadrupole spectrum requires extremely long absorption paths and a very sensitive detection system. Hertzberg (1,2) and Rank and Wiggens (3) have been able to observe several electric quadrupole transitions in the hydrogen vibration-rotation spectrum using photographic detection with long exposure times.

Although homonuclear molecules do not give rise to electric dipole infrared transitions, such molecules do possess a Raman spectrum. Rasetti (4) observed the Raman spectrum of N_2, O_2, and H_2. More recent Raman work by Stoicheff (5) has provided accurate molecular constants for the hydrogen molecule. The use of Raman scattering as a tool for observation of the spectra of homonuclear molecules is limited by the photographic detection required because of the low intensity of Raman scattering.

In 1932 Condon (6) correctly predicted that the infrared abosorption of homonuclear molecules could be observed by placing the gas in

a strong electric field, thereby inducing an electric dipole moment through which transitions could occur. Since that time, several studies have been made by Crawford and MacDonald (7), Terhune and Peters (8), Church (9), and Brannon (10) of the H_2 and D_2 molecules using the electric field induced method.

In this technique the gas is placed between two plates kept at a high potential difference. The resultant electric field induces an electric dipole moment in the molecules and the normally forbidden infrared absorption can occur. The selection rules are the same as for the Raman effect; i.e. $\Delta v = 0,1,2 - - -$; $\Delta J = 0, \pm 2$.

Gas pressures of several atmospheres are used to enable a high electric field to be maintained between the plates. This high pressure induces a shift in the line positions, and to obtain the true line positions, the absorption line should be observed at several pressures and the line positions extrapolated back to zero pressure. May, Degen, Styland and Welsh (11) studied the pressure shifts of the pure rotation spectrum of hydrogen and found a positive shift in frequency proportional to the square of the density for very high densities. The pressure shift for the pure rotation lines was found however to be very small even for high densities. From the data of May et.al.(11) the pressure shift for the pure rotation lines at the moderate densities used in this experiment would be only about .006 cm^{-1}. This was considered negligible in comparison to the expected accuracy of the line frequency determinations. The pure rotation lines in this experiment were therefore observed at only one pressure.

The pure rotation line positions of hydrogen have been studied by both Stoicheff (5) and May et. al. (11) using Raman scattering. Both measured four transitions from $S_o(0)$ through $S_o(3)$. However, the pure rotation lines have not previously been observed using the electric field induced method. The position of the $S_o(0)$ line was not determined in this experiment due to experimental difficulties, but the line positions of $S_o(1)$, $S_o(2)$ and $S_o(3)$ were determined and used to calculate the molecular constants B_o, D_o and H_o for hydrogen, and the results compared with previously obtained values.

The electric field induced technique of observing normally forbidden absorptions in homonuclear molecules is superior to the Raman scattering technique in many ways. Photographic detection is not needed, and aside from the fact that chart recording is often more convenient, the chart recording makes intensity and line shape measurements really practical even though such measurements were not made in this experiment. In addition to a high resolution infrared spectrometer only a special cell is needed to begin electric field induced work, whereas rather elaborate Raman equipment is needed.

Since the intensity of a transition in a homonuclear molecule due to an induced electric dipole moment is proportional to the square of the applied field intensity, it is important to use very high field intensities. Operational field intensity obtainable with the cell used in this work is about 200,000 volts/cm. A peak field intensity of 135,000 volts/cm was achieved in previous work with a Stark cell built by Church (9) and operated by Brannon (10). The increase in field

intensity is due to the elimination of the spacers used between the parallel plates in previous Stark cells. It is felt that this increase in field intensity made the observation of the $S_o(3)$ line possible, and of course enhanced the observation of the stronger $S_o(1)$ and $S_o(2)$ lines.

In summary, the purpose of this work was to test the performance of the new Stark cell and to observe the $S_o(1)$, $S_o(2)$ and $S_o(3)$ lines in the pure rotation spectrum of hydrogen using the higher electric field intensities. The positions of these lines were determined and the molecular constants B_o, D_o and H_o for hydrogen were calculated and compared to results previously obtained from Raman and electric field induced work.

CHAPTER II

THEORY OF ELECTRIC FIELD INDUCED ABSORPTION SPECTRA

2.1 Energy Levels of Diatomic Molecules

A diatomic molecule will absorb energy corresponding to the transitions between its quantized rotation-vibration energy states. The energy of the molecule can therefore be expressed as a sum of the vibrational and rotational energy. The rotational energy will depend on the vibrational energy state since the internuclear distance is a function of the state of vibrational excitation. This variation of the internuclear distance changes the moment of inertia which in turn effects the rotational energy. Therefore the energy of the molecule, according to Dunham (13) is:

$$T(v,J) = G(v) + F_v(J)$$

where v is the vibrational quantum number and J is the rotational quantum number.

If the molecule is assumed to be a simple harmonic oscillator, the vibrational energy would be:

$$G(v) = \omega(v+1/2)$$

where ω is the vibrational frequency in cm^{-1}. However, due to the anharmonicity of the potential function, a more accurate representation of the vibrational energy is the sum of several terms, i.e.

$$G(v) = \omega_e(v+1/2) - \omega_e X_e(v+1/2)^2 - \omega_e Y_e(v+1/2)^3 + \ldots$$

where ω_e is the harmonic vibration frequency and X_e and Y_e are constants dependent on the degree of anharmonicity of the potential function.

Forgetting for a moment that a coupling between vibrational and rotational energy exists, the energy levels of a rigid diatomic rotator are:

$$F(J) = BJ(J+1)$$

where:

$$B = \frac{h}{8\pi^2 cI} \text{ cm}^{-1}$$

h = Planck's constant

c = speed of light

I = moment of inertia

If the rigid support between the atoms is replaced with a massless spring so that centrifugal distortion may be included, the rotational energy becomes:

$$F(J) = BJ(J+1) - DJ^2(J+1)^2 + HJ^3(J+1)^3 + \ldots$$

where D and H are constants which specify the effects of centrifugal distortion on the energy of rotation.

Taking account of the effect of vibration on the internuclear distance, the rotational energy is expressed as:

$$F_v(J) = B_vJ(J+1) - D_vJ^2(J+1)^2 + H_vJ^3(J+1)^3 + \ldots$$

where:

$$B_v = B_e - \alpha_e(v+1/2) + \gamma_e (v+1/2)^2 + \ldots$$

$$D_v = D_e + \beta_e(v+1/2) + \delta_e (v+1/2)^2 + \ldots$$

$$H_v \approx H_e$$

Here B_e, D_e and H_e are constants which correspond to an equilibrum

nuclear separation, r_e, and are given by:

$$B_e = \frac{h}{8\pi^2 c I_e} \quad ; \quad D_e = \frac{4B_e^2}{\omega_e^2} \quad ; \quad H_e = \frac{48B_e^5}{\omega_e^4}$$

$\alpha_e, \gamma_e, \beta_e$ and δ_e are constants which reflect the anharmonicity of the potential function.

Combining the two expressions for the energy of rotation and the energy of vibration, the total vibration-rotation energy of a diatomic molecule is:

$$T(v,J) = \omega_e(v+1/2) - \omega_e X_e(v+1/2)^2 - \omega_e Y_e(v+1/2)^3 + \ldots$$
$$+B_v J(J+1) - D_v J^2(J+1)^2 + H_v J^3(J+1)^3 + \ldots$$

The rotational energy levels are much closer together than are the vibrational energy levels, so that the vibration-rotation energy level diagram of a diatomic molecule will appear as closely spaced rotation states superimposed on the vibrational levels.

The selection rules for allowed field induced transitions are identical to those of the Raman effect i.e.:

$$\Delta J = 0, \pm 2 \quad ; \quad \Delta v = 1, 2, \ldots$$

The Q branch corresponds to $\Delta J = 0$, the S branch corresponds to $\Delta J = +2$ and the O branch corresponds to $\Delta J = -2$. The expressions for the frequencies of the three branches are:

$$Q_v(J) = \nu_{v\to v'} + (B_{v'} - B_v) J(J+1) - (D_{v'} - D_v) J^2(J+1)^2$$
$$+ (H_{v'} - H_v) J^3(J+1)^3$$

$$O_v(J) = \nu_{v\to v'} + B_{v'}(J-2)(J-1) - B_v J(J+1) - D_{v'}(J-2)^2(J-1)^2$$
$$+D_v J^2(J+1)^2 + H_{v'}(J-2)^3(J-1)^3 - H_v J^3(J+1)^3$$

$$S_v(J) = \nu_{v\to v'} + B_{v'}(J+2)(J+3) - B_v J(J+1) - D_{v'}(J+2)^2(J+3)^2 + D_v J^2(J+1)^2 + H_{v'}(J+2)^3(J+3)^3 - H_v J^3(J+1)^3$$

where $\nu_{v\to v'} = G(v') - G(v)$. Each transition symbol completely specifies the transition in question. For example in the symbol $S_2(3)$, the S means $\Delta J = +2$, the subscript two is the final vibration state and the three is the initial rotation state. Therefore $S_2(3)$ is a transition from v = 1, J = 3 to v = 2, J = 5. A list of some of the pure rotation transitions is given in Table I. The molecular constants B_o, D_o and H_o can be calculated from these equations. Energy levels of the zero vibration state of hydrogen along with the first six allowed pure rotation transitions are shown in Figure 1. The energy levels are calculated using the molecular constants determined in this experiment.

2.2 Induced Dipole Moment

In order for a vibration-rotation transition to take place and permit absorption to occur, a molecule must possess a non-zero changing electric dipole moment; for pure rotation transitions a permanent electric dipole moment. As a general rule diatomic molecules possess a permanent electric dipole moment because of a displacement of the centers of positive and negative charge. In hetronuclear molecules the imbalance of charge produces asymmetric displacements of the centers of charge and leads to a permanent dipole moment. For homonuclear molecules however, the displacements are symmetric and produce no net dipole moment.

If the homonuclear molecules are placed in a strong electric field the centers of charge are displaced from their ordinary symmetric

TABLE I

PURE ROTATIONAL TRANSITIONS

$S_o(0) = 6B_o - 36D_o + 216H_o$
$S_o(1) = 10B_o - 140D_o + 1,720H_o$
$S_o(2) = 14B_o - 364D_o + 7,784H_o$
$S_o(3) = 18B_o - 756D_o + 25,272H_o$
$S_o(4) = 22B_o - 1,364D_o + 66,088H_o$
$S_o(5) = 26B_o - 2,236D_o + 148,616H_o$

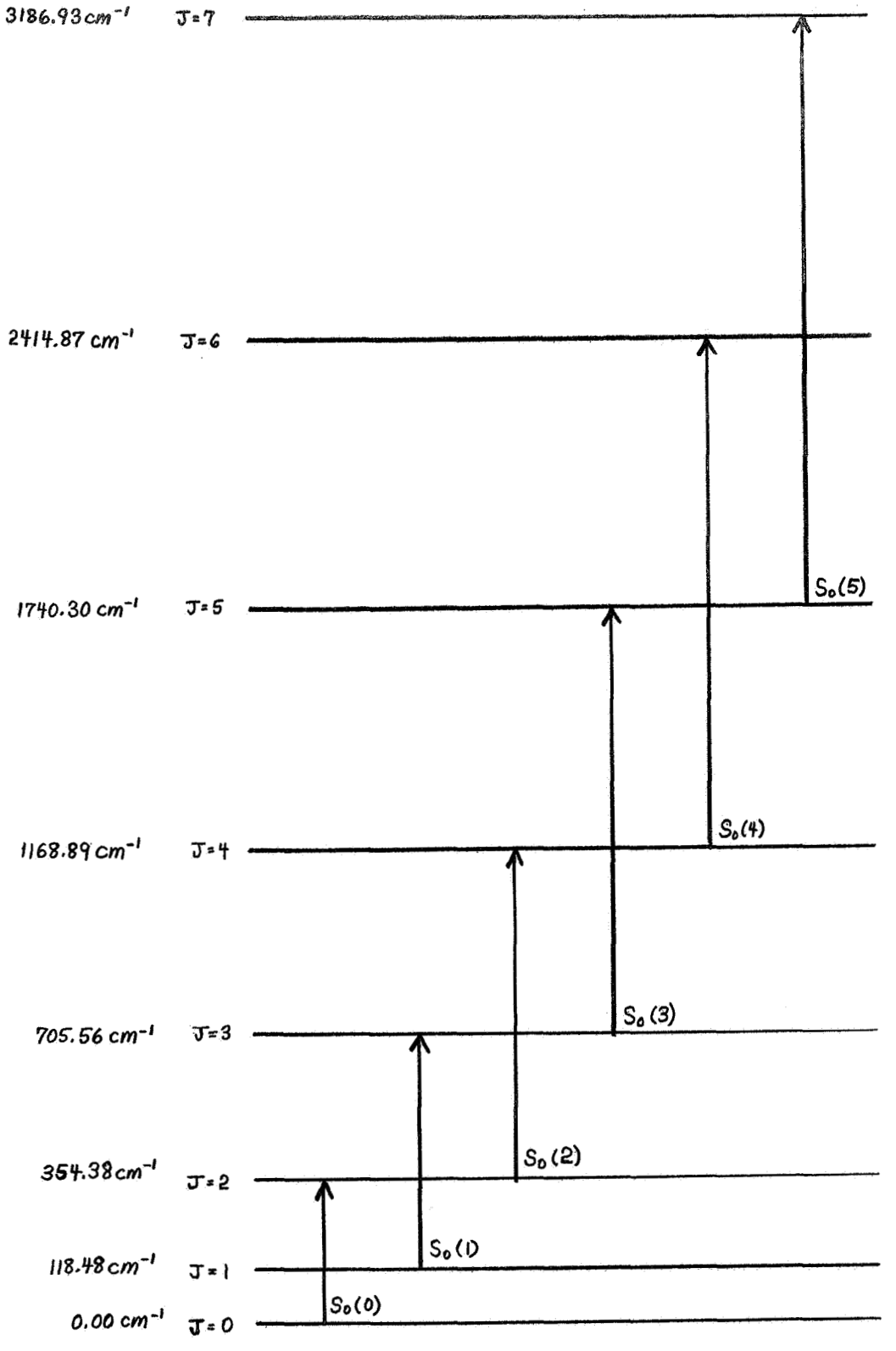

Figure 1. Pure rotational transitions of hydrogen

positions and an electric dipole moment will be induced. This allows the normally inactive electric dipole transitions to take place.

The magnitude of the induced electric dipole moment is proportional to the electric field inducing the moment:

$$\mu_i = \sum_j \alpha_{ij} E_j \qquad i = 1,2,3 \qquad j = 1,2,3$$

Here the μ_i are the components of the electric dipole moment vector, the α_{ij} are the components of the polarizability tensor, and the E_j are the components of the electric field vector. This equation is expressed in spaced-fixed coordinates taken to be X, Y, Z where Z is perpendicular to the plates and in the direction of the electric field. The coordinates $\bar{X}$, $\bar{Y}$ and $\bar{Z}$ are molecule-fixed coordinates. The molecule-fixed coordinate system is a principal axis system if the $\bar{Z}$ axis is taken along the line joining the two nuclei, and the origin is placed at the center of mass of the nuclei. The $\bar{X}$ and $\bar{Y}$ axis are interchangeable due to the cylindrical symmetry of the molecule. It is with respect to the molecule-fixed coordinates that the polarizability constants are ordinarily expressed, i.e.

$$\alpha_{\bar{x}\bar{x}} = \alpha_{\bar{y}\bar{y}} = \alpha_\perp$$

$$\alpha_{\bar{z}\bar{z}} = \alpha_\parallel$$

$\gamma = (\alpha_\parallel - \alpha_\perp)$, anisotropy of polarization

$\alpha = 1/3\ (2\alpha_\perp + \alpha_\parallel)$, average polarizability

According to Condon (6) we may transform from the molecule-fixed coordinates to space-fixed coordinates by a transformation of of the type:

$$\alpha_{ij} = \sum_{\mu\nu} a_{i\mu} a_{j\nu} \alpha_{\mu\nu}$$

The a's in this expression are obtained from the direction cosines connecting the two coordinate systems. Using the definitions of the polarizabilities, and the direction cosines we obtain for the dipole component in the space-fixed coordinate system according to Brannon(10):

$$\mu_x = \gamma \sin\theta \cos\theta \cos\phi \, E$$

$$\mu_y = \gamma \sin\theta \cos\theta \sin\phi \, E$$

$$\mu_z = \left[1/3\gamma \, (3\cos^2\theta - 1) + \alpha\right] E$$

Where θ and ϕ are the Eulearian angles connecting the two coordinate frames. The result gives the components of the dipole moment in space-fixed coordinates expressed relative to the molecule-fixed coordinate system.

2.3 Line Strength

The intensity of the absorption is dependent on the matrix elements of the induced electric dipole moment. The probability of transition is proportional to the square of the magnitude of the matrix elements of the electric dipole moment, i.e.:

$$I_{abs.} \propto \frac{1}{g_i} |\mu_w|^2$$

where g is the degeneracy and the μ are:

$$|\mu_x| = \int \psi_n^* \mu_x \psi_m \, d\tau$$

$$|\mu_y| = \int \psi_n^* \mu_y \psi_m \, d\tau$$

$$|\mu_z| = \int \psi_n^* \mu_z \psi_m \, d\tau$$

When the dipole moments from Section 2.2 are substituted into these expressions and the integrations preformed, the line strengths are obtained. The general expression for the S branch line strength, from Brannon (10), for radiation polarized perpendicular or parallel to the plates is given in Table II. The calculated line strengths for some of the pure rotational transitions are also given in Table II. It may be seen from these equations that the intensities of the lines are proportional to the square of the electric field intensity, and for this reason it is important to obtain as great a field intensity as possible.

2.4 Integrated Absorption

The final intensity of a transition is dependent on the number of molecules in the initial state. The intensity of a line depends on the Boltzmann factor f_{vj}, where:

$$f_{vj} = \frac{(2J + 1)\, g(J)\, e^{-W_{vj}/KT}}{\sum g(J)\, (2J + 1) e^{-W_{vj}/KT}}$$

W_{vj} is the energy of the state and g(J) is the spin degeneracy. The Boltzmann factor for some of the pure rotational transitions is given in Table III for T = 300°K.

TABLE II

LINE STRENGTH OF PURE ROTATION TRANSITIONS

$$\left(S^{J+2,\ v'}_{J,v}\right)_{\parallel} = \frac{2}{15}\frac{(J+1)(J+2)}{(2J+3)(2J+1)} \gamma_{vv'}^{2} E^{2}$$

$$\left(S^{J+2,\ v'}_{J,v}\right)_{\perp} = \frac{1}{10}\frac{(J+1)(J+2)}{(2J+3)(2J+1)} \gamma_{vv'}^{2} E^{2}$$

Transition	Line Strength notation	Line Strength
$S_o(0)$	$\left(S^{2,o}_{o,o}\right)_{\parallel}$	$.0889\ \gamma_{oo}^{2} E^{2}$
$S_o(0)$	$\left(S^{2,o}_{o,o}\right)_{\perp}$	$.0667\ \gamma_{oo}^{2} E^{2}$
$S_o(1)$	$\left(S^{3,o}_{1,o}\right)_{\parallel}$	$.0533\ \gamma_{oo}^{2} E^{2}$
$S_o(1)$	$\left(S^{3,o}_{1,o}\right)_{\perp}$	$.0400\ \gamma_{oo}^{2} E^{2}$
$S_o(2)$	$\left(S^{4,o}_{2,o}\right)_{\parallel}$	$.0457\ \gamma_{oo}^{2} E^{2}$
$S_o(2)$	$\left(S^{4,o}_{2,o}\right)_{\perp}$	$.0343\ \gamma_{oo}^{2} E^{2}$
$S_o(3)$	$\left(S^{5,o}_{3,o}\right)_{\parallel}$	$.0423\ \gamma_{oo}^{2} E^{2}$
$S_o(3)$	$\left(S^{5,o}_{3,o}\right)_{\perp}$	$.0317\ \gamma_{oo}^{2} E^{2}$
$S_o(4)$	$\left(S^{6,o}_{4,o}\right)_{\parallel}$	$.0404\ \gamma_{oo}^{2} E^{2}$
$S_o(4)$	$\left(S^{6,o}_{4,o}\right)_{\perp}$	$.0303\ \gamma_{oo}^{2} E^{2}$
$S_o(5)$	$\left(S^{7,o}_{5,o}\right)_{\parallel}$	$.0378\ \gamma_{oo}^{2} E^{2}$
$S_o(5)$	$\left(S^{7,o}_{5,o}\right)_{\perp}$	$.0294\ \gamma_{oo}^{2} E^{2}$

TABLE III

BOLTZMANN FACTOR FOR PURE ROTATION TRANSITIONS

Transition	Boltzmann Factor (f_{vj})
$S_o(0)$	0.1294
$S_o(1)$	0.6592
$S_o(2)$	0.1173
$S_o(3)$	0.0894
$S_o(4)$	0.0039
$S_o(5)$	0.0008

The total integrated absorption is, according to Brannon (10),

$$(A)_{\parallel \text{ or } \perp} = (1.018 \times 10^{35}) \frac{LPE^2}{T} f_{vJ} \nu_{vJ}^{v'J'} \left(S_{vJ}^{v'J'}\right)_{\parallel \text{ or } \perp}$$

Where L is the absorption path length in cm., P is the pressure in atmospheres and ν is the frequency in cm^{-1}. The product of the last three terms gives the characteristic relative intensity of a particular line while the other terms depend on the experimental conditions. Table IV gives this product for some of the pure rotational transitions normalized to the value of the $S_o(1)$ transition. The rapid fall off in absorption is seen past J=3, and these lines would be difficult to observe. The peak absorption height for the $S_o(1)$ hydrogen line observed in this experiment was about 10%; for the $S_o(2)$ line about 6%; for the $S_o(3)$ line about 4%.

TABLE IV

RELATIVE INTENSITIES OF PURE ROTATION TRANSITIONS

Transition	Relative Intensity
$S_o(0)$	0.198
$S_o(1)$	1.000
$S_o(2)$	0.212
$S_o(3)$	0.189
$S_o(4)$	0.010
$S_o(5)$	0.002

CHAPTER III

EXPERIMENTAL APPARATUS AND TECHNIQUES

3.1 The Stark Cell

The Stark cell contains two accurately parallel chrome plated steel plates which are maintained at a high potential difference, creating a strong electric field in the gap between them. The sample gas is used at high pressures to increase the potential difference which can be maintained between the parallel plates, and so the cell must be able to withstand these high pressures. The present cell operates at 400 p.s.i. and the operating field intensity is about 200,000 volts/cm. The peak field intensity achieved in hydrogen just before breakdown is 240,000 volts/cm. at 400 p.s.i. In nitrogen compressed to 400 p.s.i. the peak field intensity achieved is 350,000 volts/cm. These field intensities are higher than those previously obtained in a cell of this type.

In 1953 Crawford and Dagg (13) used a parallel plate arrangement separated by lucite spacers and achieved an electric field intensity of 100,000 volts/cm. in hydrogen at pressures up to 2,000 p.s.i. In 1958 Crawford and MacDonald (7) used a similar arrangement and obtained field intensities of 130,000 volts/cm. in hydrogen at 1,500 p.s.i. Terhune and Peters (8) in 1959 used a concentric cylinder electrode configuration with lucite spacers and obtained an electric field intensity of 100,000 volts/cm. in hydrogen at 600 p.s.i. Church (9) in 1959 and Brannon (10) in 1965 using parallel plates with plexiglas

spacers obtained field intensities of 100,000 volts/cm. and 130,000 volts/cm. respectively in hydrogen at 550 p.s.i. In 1966 Foltz, Rank and Wiggens (14) again using parallel plates, obtained field intensities of 90,000 volts/cm. in hydrogen at 1,100 p.s.i. The literature does not indicate whether plastic spacers were used between the plates, but the field intensity achieved strongly suggests this.

Common to each of these cells is the use of plastic spacers between the electrodes, and this is the factor which limits the voltage across the electrodes. It has been shown (15) that the AC or DC breakdown voltage across the surface of many insulating materials (including lucite) placed between parallel plates in a compressed gas is less than if the material was not present. Under ideal conditions with no insulating material between the parallel plates, it has been shown (15) that for the value of the product of pressure and plate spacing corresponding to the parameters of the new Stark cell, the breakdown voltage across hydrogen would be 70,000 volts. This corresponds to a field intensity of about 440,000 volts/cm.

The present Stark cell was tested with quartz and Mylar spacers with no significant improvement over previously achieved field intensities. However, with the elimination of the spacers, operating field intensities of 200,000 volts/cm. are easily obtainable in hydrogen at 400 p.s.i. across a 1/16 inch gap. The peak field intensity achieved to date just before breakdown is 240,000 volts/cm. at

these same conditions.

The gas cell is shown in Figure 2, Figure 3 and Figure 4. The plates are chrome plated steel, two inches wide and 1/2 inch thick. The edges and ends of the plates are rounded, as are all metal surfaces inside the cell, to prevent breakdown or energy losses due to corona discharge. Each plate is attached to a plexiglas holder with nylon screws. The holder when assembled keeps the plates 1/16 inch apart with no spacers between them. Four separate holder assemblies were made for plate lengths of 11, 17, 23 and 35 inches. These assemblies fit into the high pressure cell which is made in 6, 12 and 24 inch sections. The sections are interchangeable and bolt together to give the desired cell length. Plexiglas cemented inside the cell serves as a track to position the plate assembly and also reduces the volume of the cell. The end caps shown in Figure 3 fit onto any length cell and hold the high voltage connector, windows and the sample gas inlet and outlet. The high voltage connector shown in Figure 5 is a brass rod passing through a machined nylon insulator. A rounded plug from the connector fits into a socket attached to the high voltage plate, while a spring grounds the other plate. This allows the end caps to be removed easily without removing the plates. O-rings seal the connector gas tight. Several connectors machined of polystyrene could not withstand the shear forces created in tightening the nut used to seal the connector.

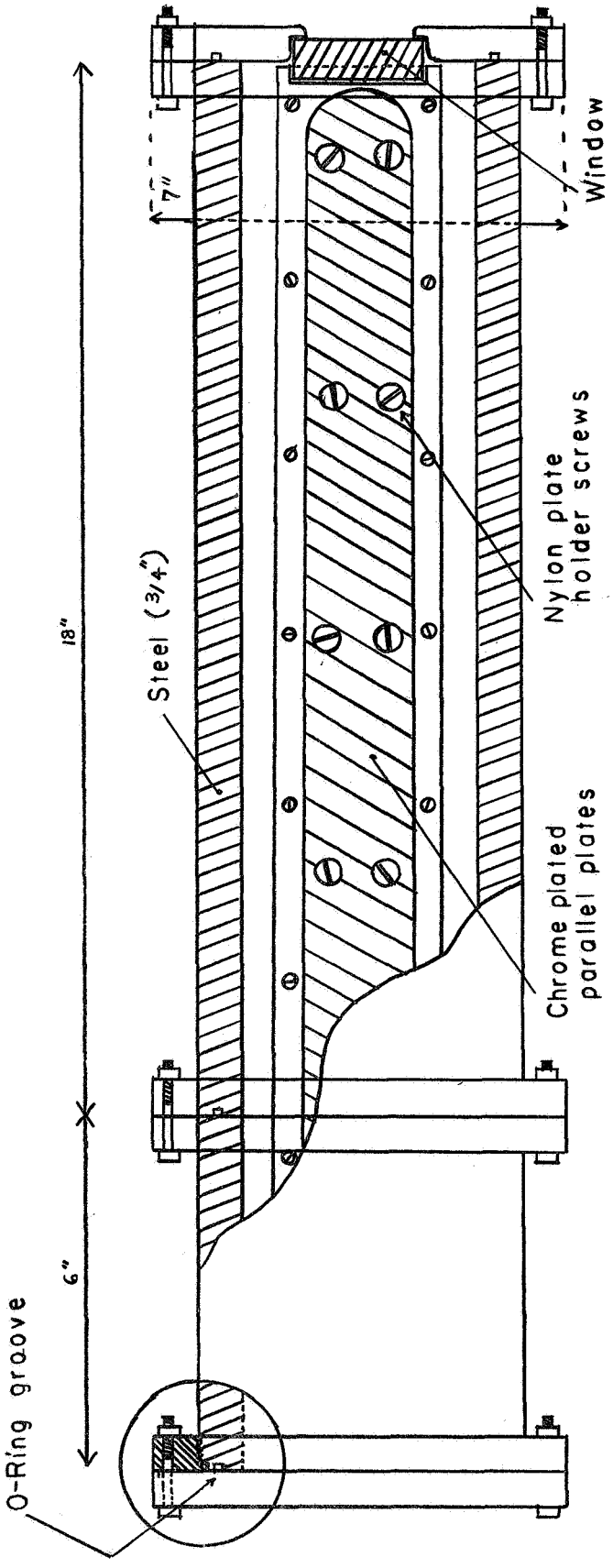

Figure 2. High pressure Stark Cell

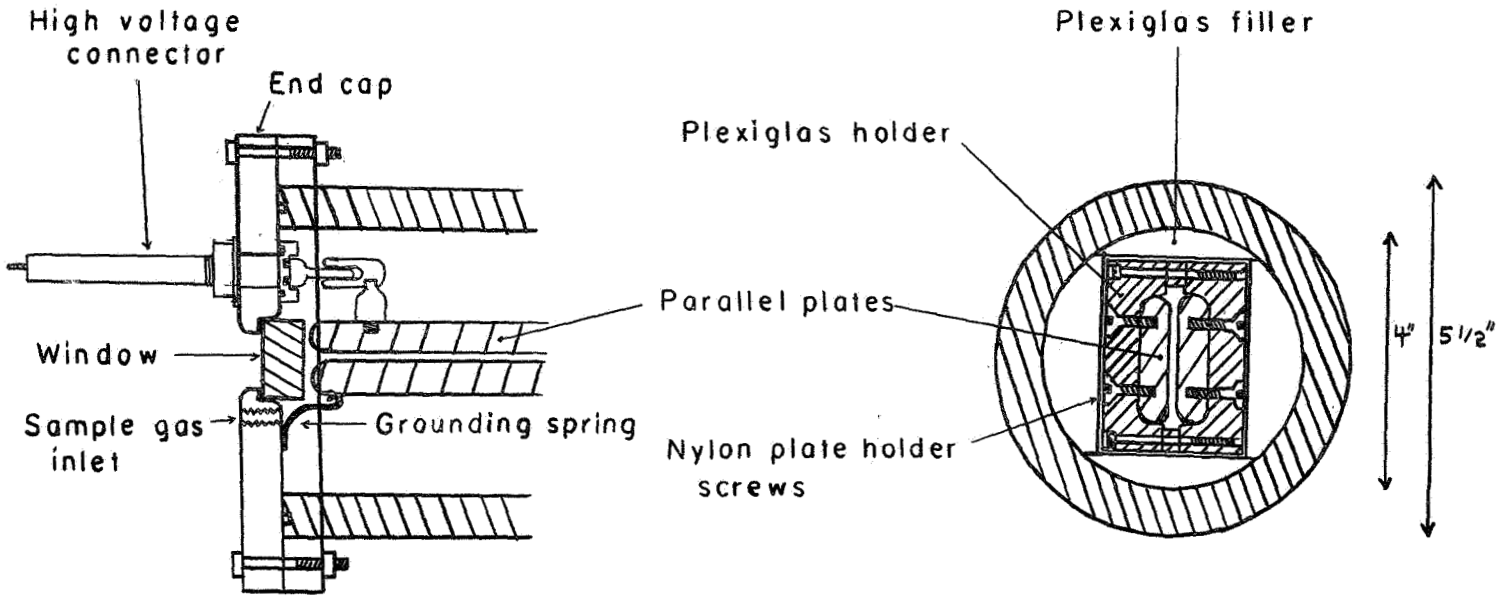

Figure 3. End cap detail

Cross sectional view

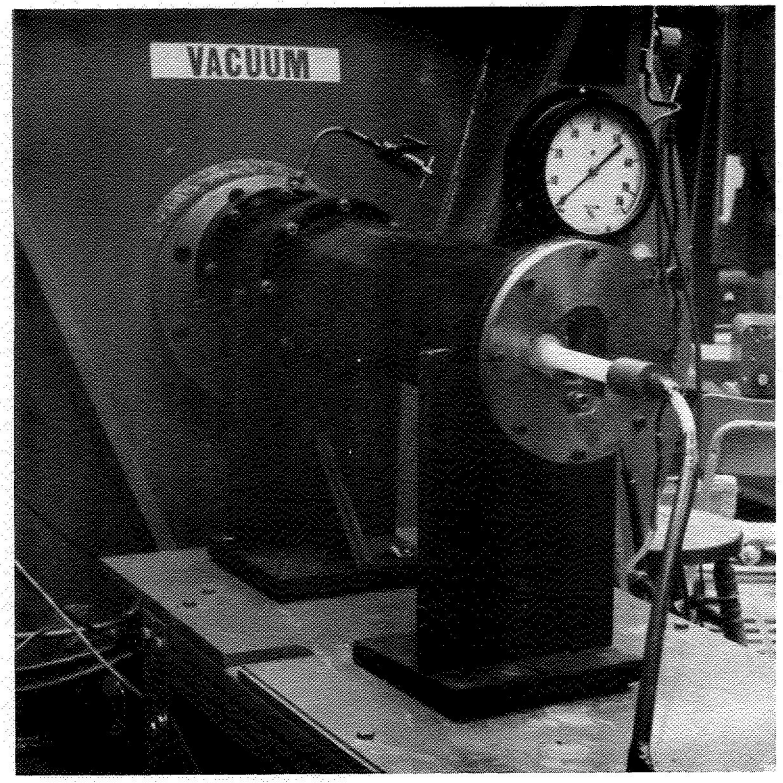

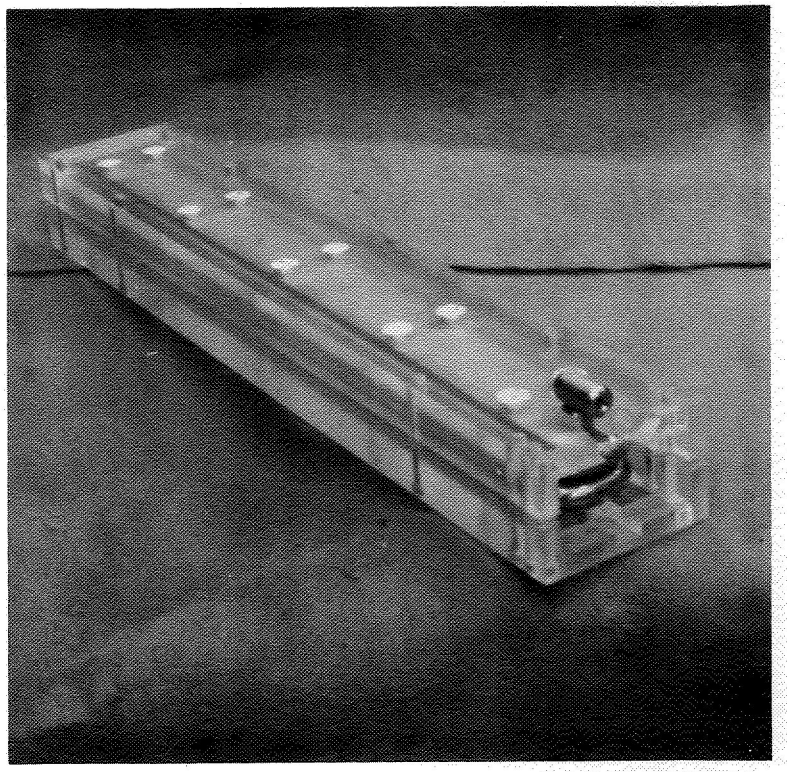

Figure 4. Cell and plate holder assembly

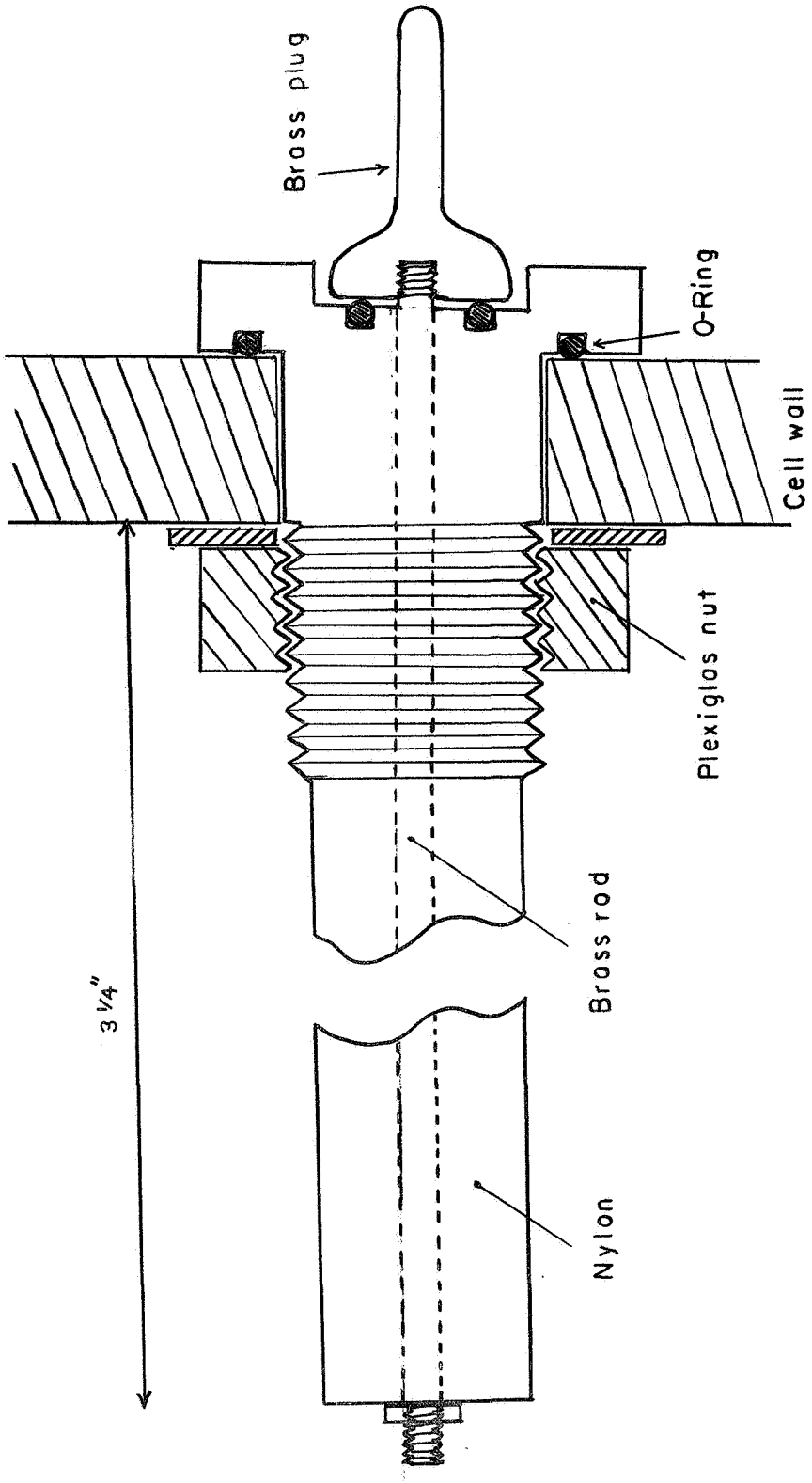

Figure 5. High voltage connector

As mentioned before, the cleanness of the plate is an important factor in obtaining high field intensities. To clean the plates, the plate holder is disassembled and the plexiglas holders cleaned with soap and water and rinsed thoroughly. The plates themselves are first cleaned in acetone with a soft cloth and then in pure ethyl alcohol. Gloves are used with the final alcohol cleaning. When the plexiglas holders are thoroughly dry, the assembly is put back together using gloves. The entire assembly is then stood upright in a container, and alcohol is poured down the plates. In order to remove any dust which may be clinging to the plates due to an electrostatic charge, 1/8 inch brass rods thoroughly cleaned are inserted down each side of the plates their whole length and placed so that they touch both plates. This approximates a closed hollow conductor so that the charge resides on its outside surface and allows the alcohol to wash away these stubborn dust particles. The assembly is allowed to dry thoroughly before replacing in the cell.

"Aging" the plates by allowing them to breakdown for short periods and then recleaning them appreciably increases the field intensities which can be achieved. This has been observed before (15) and serves to burn off small irregularieties and high spots on the plate surface. The "aging" process is thought to be limited by the small pits which the discharge creates. These pits even with their associated sharp edges should, however, break down at a higher voltage than the high spot which was burned off.

Since the cell cannot be evacuated due to the window configuration, it must be flushed before filling. The air in the cell is first flushed out with nitrogen to prevent an explosive air hydrogen mixture in the closed cell. Hydrogen is then used to flush the gas lines and cell of nitrogen and is burned off as it leaves the cell. When the lines are clear of nitrogen a liquid nitrogen cold trap is placed in the hydrogen line to remove the water from the gas, and the flushing process is continued. The hydrogen line to the cold trap is left open a few minutes after the cell is brought up to the operating pressure to freeze out any remaining water. The cell valve is then closed to isolate the cell. The pressure is read with an accurate U.S. Gauge pressure gauge. Pressures of 400 p.s.i. were used in all data included in this work.

The window arrangement used in the cell end caps was unsatisfactory. The 5/8 inch thick windows were originally sealed in place with silicone rubber. The positive pressure in the cell forces the window down forming the seal. It was found however that the silicone rubber was forced out from under the window leaving the center of the window unsupported. This lead to a gradual bending of the window and pressure leaks. A rubber gasket under the window held in place with silicone rubber gave the same trouble. A cork gasket under the window sealed with silicone rubber was more rigid and lasted longer but would eventually blow out causing a leak in the cell. A more satisfactory arrangement would use double O-rings; one on each side of the window. The O-rings would provide a better seal, and the double

O-ring would allow the cell to be evacuated. The windows would also be easy to change.

Potassium bromide windows were used in the cell for the $S_o(1)$ hydrogen line, and sodium chloride windows were used for the $S_o(2)$ and $S_o(3)$ lines. A 100 watt light bulb was placed near the exposed cell window to keep its ambient temperature above that of the room and prevent the window from fogging.

3.2 High Voltage Supply

The high voltage to the Stark cell was supplied by a 75,000 volt transformer power supply from Plastic Capacitor, Inc., Chicago, Ill. The voltage to the cell is adjusted by a variac on the primary side of the transformer. The voltage is measured through a 1,000 megohm resistor in series with an 80 microamp Simpson meter calibrated at 80,000 volts full scale. A 22 megohm series resistor in the high voltage line to the cell prevents currents greater than the rating of the power supply in the event of breakdown across the plates. The current rating of the power supply is five milliamps. Occasionally when the wattage rating of this resistor was exceeded during breakdown, the resistor would explode and therefore acted like a fuse. An ordinary fuse burned out every time the plates broke down and therefore could not be used. The breakdowns have so far not noticeably affected the performance of the power supply.

Breakdown across the plates was not uncommon. In the "aging" process this was done deliberately for short periods of time. Due

to window problems the cell was occasionally operated with slow pressure leaks. When the pressure drops the cell will of course breakdown. If the cell was opened, the plates would breakdown several times when the voltage was turned on again. This is due to dust which entered the cell. Apparently this process destroys the particles since the voltage can then be turned up to the ordinary operating voltage. The normal operating voltage was 40,000 volts.

3.3 Infrared Source

A carbon rod furnace infrared source shown in Figure 6 and Figure 7 built for this experiment has proven to be a very reliable and trouble-free source despite high operating temperatures of $2,600^{o}$ Kelvin and large power requirements. Its high operating temperature provides usable energy out to about 40 microns and the emissivity of the rod is very close to unity. The rod is slotted in the center to increase the resistance of this portion of the rod and therefore increase the temperature.

The source was built with reference to designs by Spaunbauer (16) and Wiggens (17) in an effort to combine the best features of both as well as to make improvements to increase the operating temperature.

The carbon rod used in the source is spectroscopically pure, 5/16 inches in diameter and 3-3/4 inches long. The rods are slotted in the center a length of 1-1/2 or 2 inches depending on the slot configuration. The pure carbon proved much superior to ordinary grade carbon such as is used in welding. These rods contain oil and

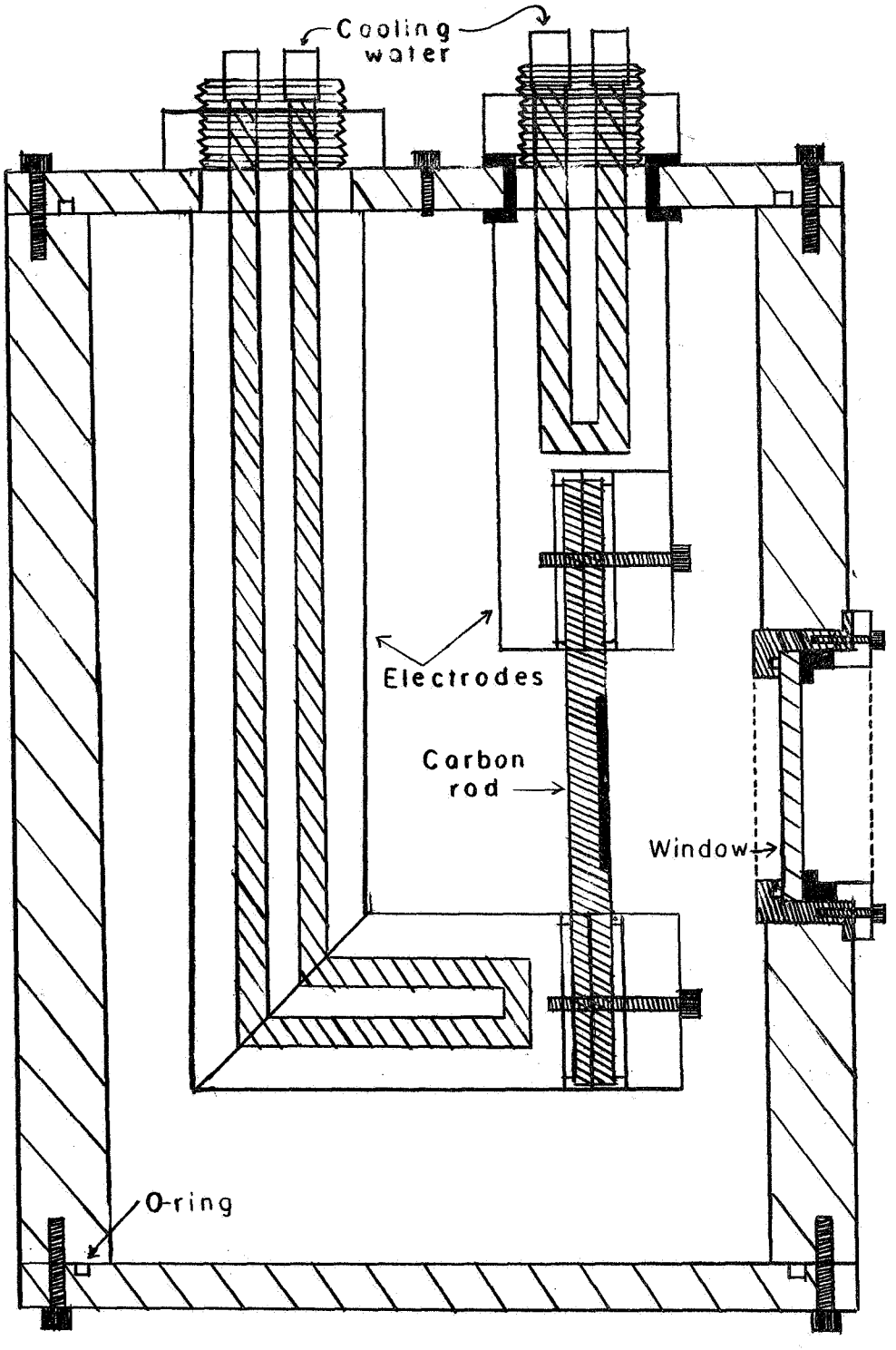

Figure 6. Carbon rod furnace

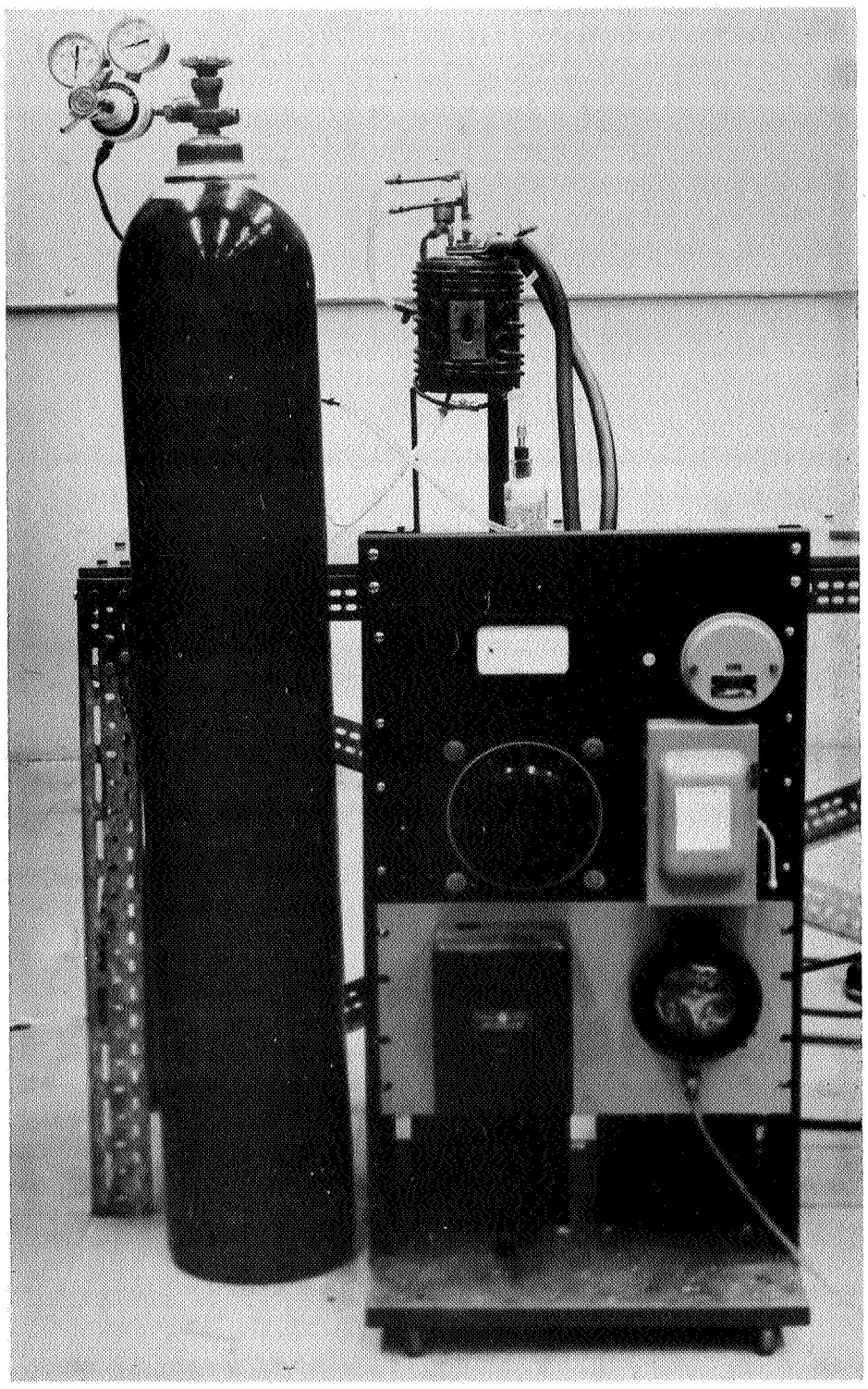

Figure 7. Carbon rod furnace with gas and power supply

binder materials which smoke as the rod is heated. Two different slot configurations were tried; a rectangular cross section slot and a V-cross section slot. The rectangular slot gave off slightly more energy (about 15%) than the V-slot rod but the small sacrifice in energy was more than compensated for in the longer life of the V-slot configuration. The useful life of the V-slot rods was about 100 hours; the life of the rectangular slot only about 40 hours. Another advantage of the V-slot is that a slight misalignment in the rotational placement of the rod in its holder should make no difference. The V-slot was made with a 60^{o} cutter to a depth of 0.110 inch. The ends of the two inch long slot are not this deep but only the center one inch portion is used as a source.

The rod is held in place by two, one inch diameter copper electrodes. The electrodes carry power to the rod and are water cooled through holes drilled axially. The right angle electrode is silver soldered at its joint mainly for strength rather than temperature considerations.

The electrodes and carbon rod are encased in a water cooled case. This was accomplished simply by wrapping the cylindrical case with copper tubing and soft soldering to provide good thermal contact. The top and bottom of the case are also cooled with tubing wrapped circularly and connected to the cooling coils on the side.

The case is flushed with argon before the rod is heated and kept at about 3 p.s.i. positive pressure (gauge) while the rod is operating.

In order to eliminate problems from a small amount of water in the argon, the gas was dried by passing it through a drying agent before entering the case.

The window and window holder were the only troublesome features. The first window holder made, used flat rubber gaskets as seals. These gaskets were exposed to the radiation coming through the window, and quickly carbonized and allowed the case to leak. Even when the gaskets were shielded with aluminum foil to prevent the carbonizing, the flat gaskets continued to leak as often as not. Both problems were solved simultaneously and satisfactorily by making a new window holder shown in Figure 6 which was soft soldered into the case. The seal at the window is made by an O-ring placed in a rectangular slot around the window opening. The window is pressed against this O-ring by a spacer which is pressed against the window by a plate bolted to the front of the holder. Different spacers allow different window thicknesses to be used.

One problem which persists occasionally is window breakage, due to the high temperatures. However, if the source is heated and cooled slowly, the number of windows broken can be kept to a minimum. The most reliable window material seems to be sodium chloride, which is better able to withstand the high temperatures and temperature changes. To keep window fogging to a minimum, a 100 watt light bulb is placed in front of the window to keep its temperature above the ambient temperature of the room, when the furnace is not operating.

The inside surface is kept clear by the drying agent in the argon line.

For the preliminary work in the fundamental region, a commercial quartz iodine lamp with an advertised temperature of 3,000° Kelvin was a very satisfactory source.

3.4 High Current Power Supply

The power supply for the carbon rod furnace infrared source shown in Figure 8, is made up of two, six volt transformers rated at 500 amps, connected in series. The 220 volt primary voltage is controlled by a large variac rated at 22 amps. The current in the secondary is measured by a current transformer and Simpson meter calibrated to read 500 amps full scale. Normal operating current through the carbon rod is 400 amps.

Ordinary welding cable rated at 400 amps was not large enough to handle this current continuously, and became very hot during operation. A larger cable with a wire diameter of 3/4 inch operated much cooler and consequently took less power away from the rod. Large lugs soldered on the ends of the cable make the connection at the power supply and source.

A safety feature added to the power supply automatically turns off the power to the source in case the water is turned off or drops significantly in pressure, while the furnace is operating. Also the rod cannot be turned on without turning on the water. A pressure

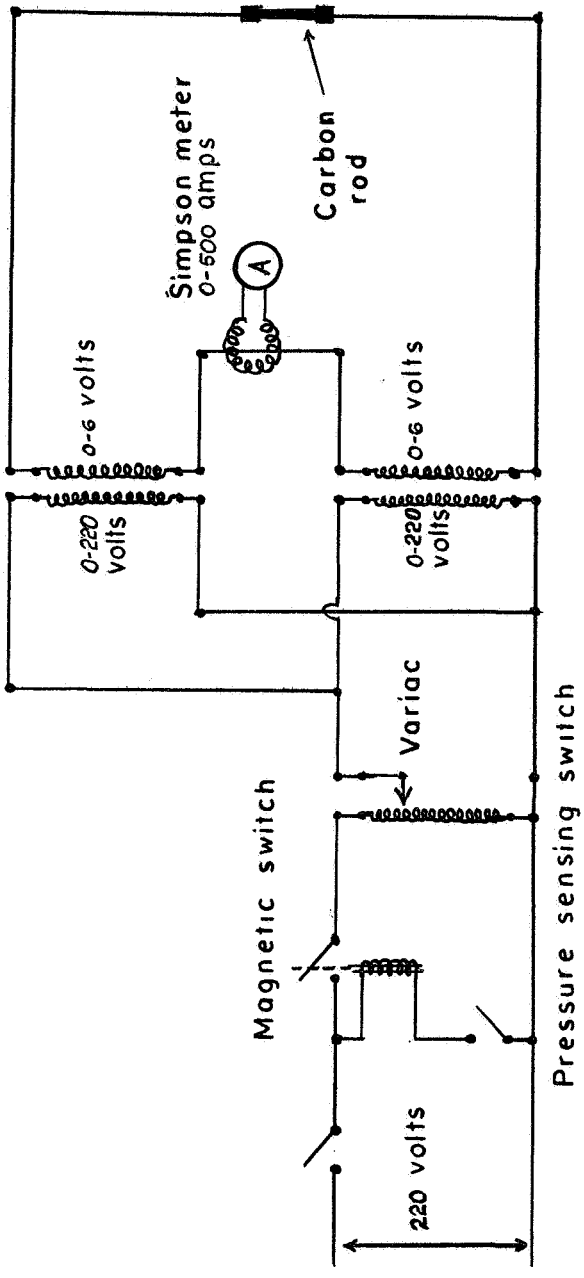

Figure 8. High current power supply

sensing Mercoid switch is tripped when the cooling water is turned on. This completes the circuit to a heavy duty magnetic starter switch which is then closed to apply voltage to the primary. If the water pressure changes significantly the Mercoid switch opens, opening the magnetic starter switch which automatically turns off the power to the carbon rod source before any damage can occur.

The operating procedure is more complicated than that used with conventional sources. The case is first flushed with argon and the pressure adjusted to about 3 p.s.i. positive pressure. The gas line is kept open since the case leaks slightly. The main switch is turned on with the variac set at zero. This is necessary since the Mercoid switch derives its power from the incoming voltage. The water is turned on to a preset pressure which closes the Mercoid switch. Closing the Mercoid switch completes the circuit to the magnetic starter switch which puts power on the primary. The variac is then turned up until the current in the secondary is 150 amps, which starts the rod. The variac is then turned up slowly in 25 amp intervals over a period of about five minutes to give the window ample time to adjust to the temperature change, until the operating current of 400 amps is reached. The voltage at the rod after line losses have occurred is about 10.5 volts. The operating temperature of the rod at these conditions is about 2,600^{o} Kelvin as measured with an optical pyrometer. Figure 9 shows the energy of the carbon

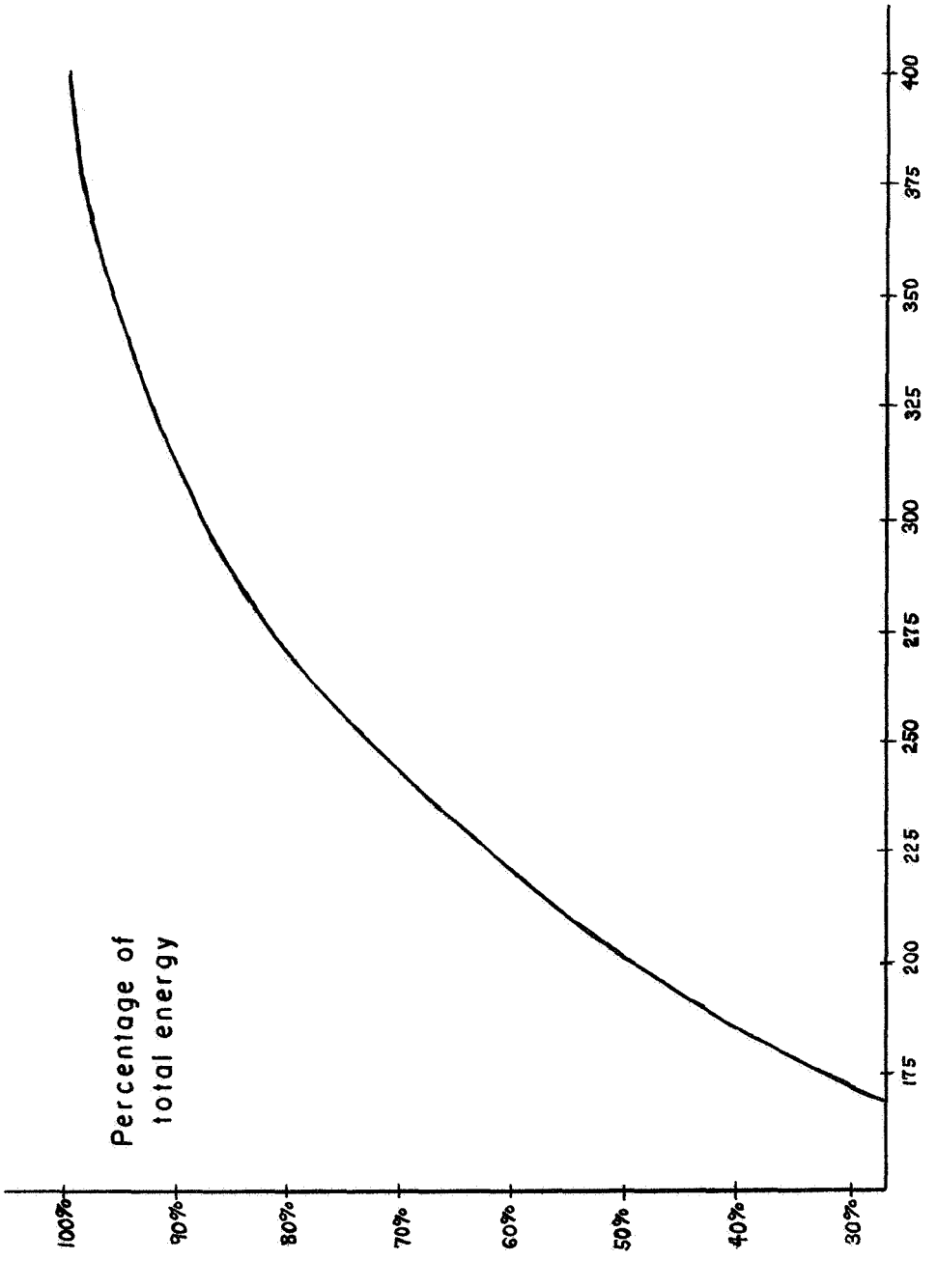

Figure 9. Energy of the carbon rod as a function of the rod current

rod at the detector as a function of the rod current at a wavelength of about 4.5 microns.

3.5 Spectrometer and Optics

The vacuum-grating spectrometer used in this experiment was built in 1957 and is described by Herndon, Deeds, Gailar, Herget, Lovell and Nielsen (18). The fore optics were changed in order to be able to use the Stark cell outside the spectrometer. The cell was operated outside the spectrometer for several reasons:

1. The danger of explosive hydrogen leaking from the cell into the tank. This represents no danger in a vacuum but when air is admitted into the tank as it is opened, an explosive mixture could result.
2. The danger of a spark jump from the high voltage connector in a vacuum.
3. The original sample cell area optics did not allow enough room for the cell.
4. Convenience in refilling and working on the cell.
5. The detector for the pure rotational lines could not be operated efficiently in a vacuum.

The cell was placed outside the spectrometer on a table with the infrared source and mirror to focus the radiation on the end of the plates. The cell was fastened to a port on the spectrometer bulkhead with a plate made for that purpose, and sealed with O-rings.

The radiation from the carbon rod is collected by M1 and focused onto the end of the plates through the cell windows as shown in Figure 10. M1 magnifies the image by two, and the beam is f-10 as it enters the plates. The radiation is transmitted wave guide fashion by the plates and is allowed to diverge as it strikes M2, M3 and M4, shown in Figure 11. These flat mirrors provide a long path to M5 so that the beam may be reduced 2:1 as it enters S1, the entrance slit to the fore optics. The spectrometer originally had a monochrometer system which was modified in 1962 to remove the prism in favor of using band pass filters. The filters were tried but proved to be inadequate in separating the orders of the grating. The prism was therefore put back in and realigned.

The prism mirror drive which selects the radiation passed by the prism is not calibrated in wave numbers and so a scheme had to be devised to find the position of the desired radiation. This was accomplished by observing the angular position of the grating orders near central image. For example, if it were desired to pass 10 micron radiation, the grating equation was used to calculate the angle at which 10 micron radiation from the grating was diffracted in, for example, fourth order. The prism mirror was then adjusted as the orders were run until the fourth order coincided with the calculated angle. The prism is then passing 10 micron radiation. The reading on the prism mirror dial can then be recorded for future use of that

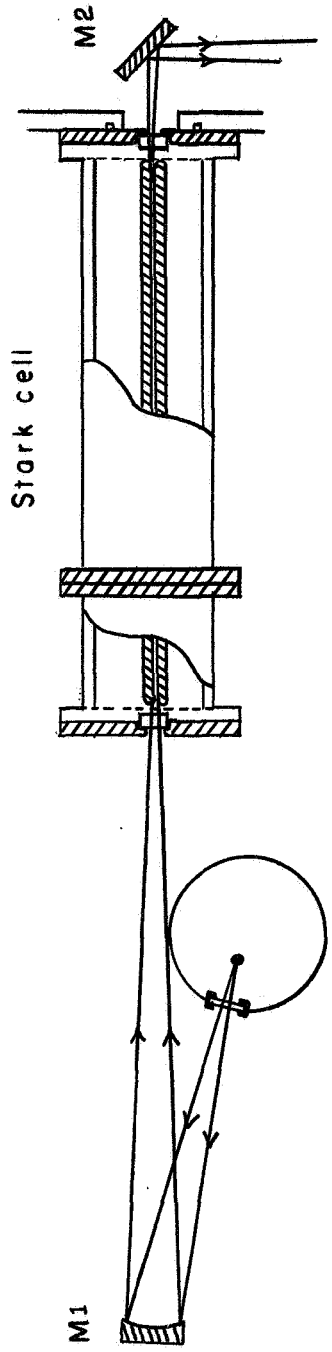

Figure 10. Infrared source and Stark cell

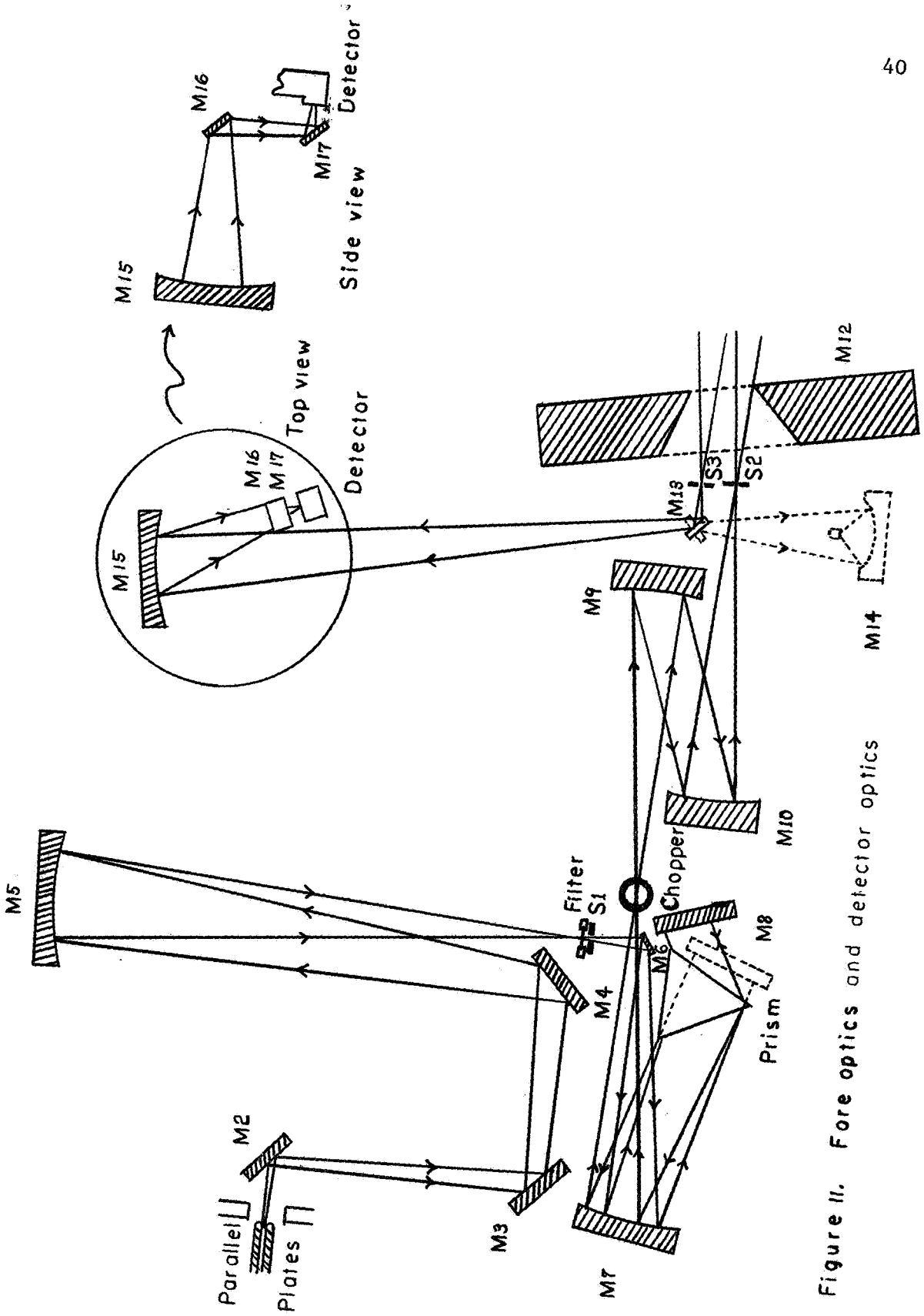

Figure 11. Fore optics and detector optics

setting. A potassium bromide prism was used for the $S_o(1)$ line while sodium chloride was used for the $S_o(2)$ and $S_o(3)$ lines.

The grating optics shown in Figure 12 were not changed with the exception of realignment and focusing. Several gratings were tried. For the fundamental an eight inch grating with 600 grooves per m.m. was used in first order. For the pure rotation lines a 30 groove per m.m. grating blazed at $63\text{-}1/2^{o}$ was used. The pure rotation lines were observed in fifth, fourth and third orders of this grating in order of decreasing wave number. The carbon monoxide calibration lines appeared in the tenth and eleventh orders. The spectral slit width for the $S_o(1)$ line was $.08cm^{-1}$, for the $S_o(2)$ line, $0.1cm^{-1}$, and for the $S_o(3)$ line, $0.2cm^{-1}$.

3.4 Detector

An uncooled Santa Barbara Research Center lead sulfide detector was used in preliminary work with the fundamental of hydrogen. As the work was subsequently directed to the pure rotation lines, a thermocouple by Charles M. Reeder was installed in place of the lead sulfide detector. The thermocouple was, however, not sensitive enough in the energy limited region of the pure rotation lines, and was replaced by a copper-doped germanium, liquid helium cooled Santa Barbara Research Center detector. This detector with its cryostat was not designed to fit into the present spectrometer, and a holder had to be made to hold it in place. A simple three post holder was

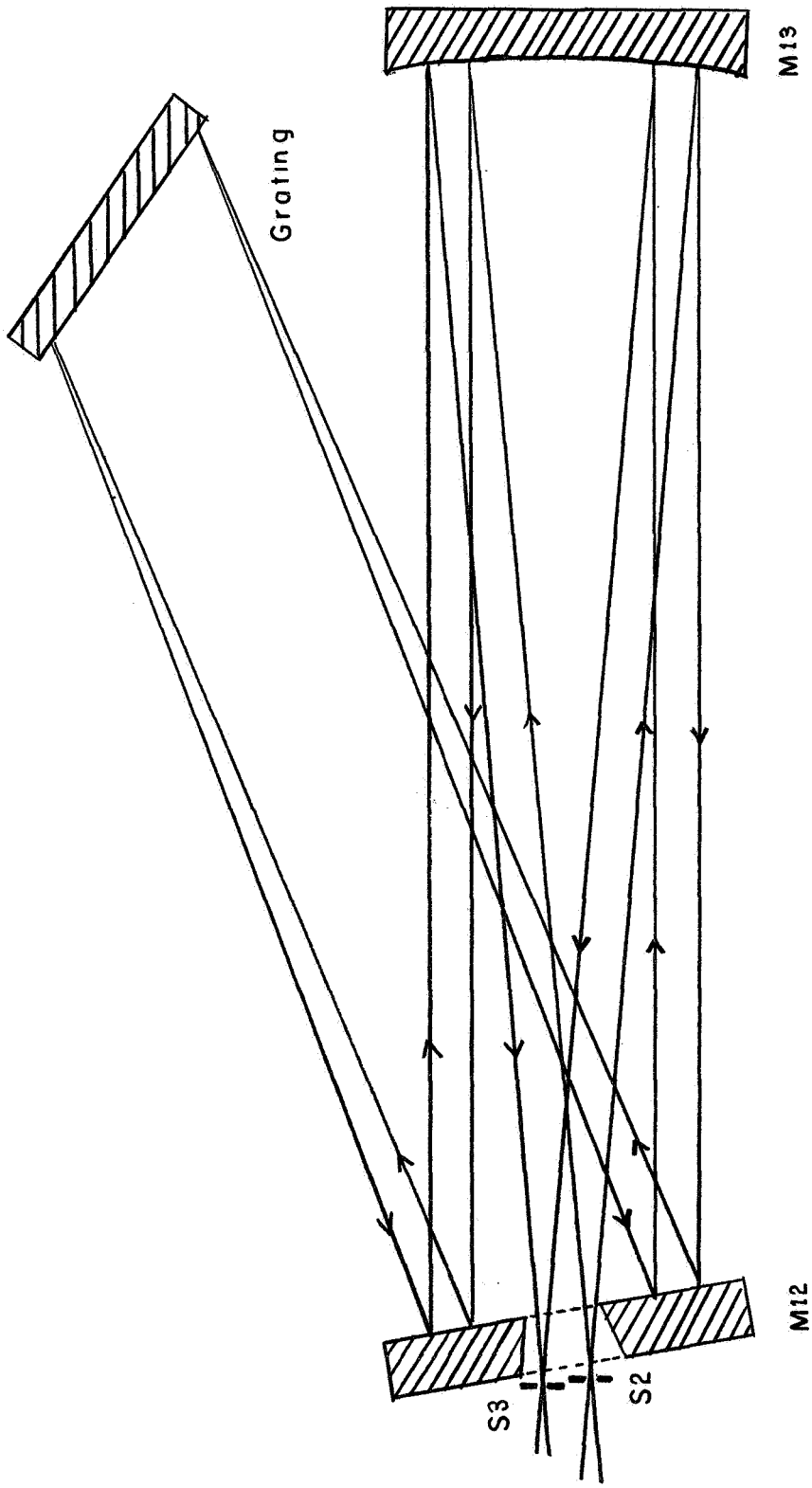

Figure 12. Grating optics

made and the detector optics changed to direct light into the detector as shown in Figure 11 on page 40. This involved dropping the optical axis because of the height of the detector cryostat. A potassium bromide window was used in the detector for all work with the pure rotational lines.

The copper-doped germanium detector was about eight times as sensitive as the thermocouple and made detection of the lines possible, but created its own problems. The liquid helium hold time in the detector was only about two hours which lead to a rather heavy use of liquid helium. The short hold time also meant that the lines had to be run in air, since the spectrometer tank takes over two hours to evacuate. The detector dewar uses a vacuum insulation which must be repumped if the dewar is allowed to warm up. After the vacuum insulation has been evacuated, the dewar must be prechilled with liquid nitrogen which is poured out before the liquid helium can be put in. With all the time spent in preparation of the dewar to accept the liquid helium, it was necessary to keep liquid helium in the detector until the supply was gone. With a hold time of only two hours this meant working 24 hours a day as long as the liquid helium lasted.

It is felt that the short hold time in the dewar is due to insufficient vacuum in the vacuum insulation. The average pressure used was 6×10^{-4} Torr.

3.5 Electronics

The copper-doped germanium detector was biased with a 45 volt battery in series with a 7.5 kilohm resistor and a 5 kilohm variable potentiometer. The detector bias current was monitored on a five milliampere Simpson meter and adjusted to the recommended three milliampere bias current. These components were shielded in a metal box to eliminate any pick-up problems.

A 600 c.p.s. barrel type chopper was used both with the copper-doped germanium detector and the lead sulfide detector. The signal was amplified by a Princeton Applied Research Type A preamplifier and HR-8 lock in amplifer. The amplified signal was recorded by a single pen Mosely recorder.

CHAPTER IV

EXPERIMENT AND OPERATING CONDITIONS

The hydrogen fundamental vibration-rotation spectrum was run as a preliminary check on the cell and spectometer. The lines were run using the quartz iodine lamp as an infrared source, the 600 grove per m.m. grating, the 2-4 micron band pass filter to separate the orders of the grating and the uncooled lead sulfide detector. All of these components have been discussed in the previous sections.

After calibrating the grating with CO and HF lines, the hydrogen fundamental lines were found easily. To determine if a suspect line is really a hydrogen line is easy under ideal conditions; i.e. plenty of energy, strong lines, and good signal to noise ratio. It is not enough merely to turn off the field and observe if the lines disappear. The field can cause some shift in the positions of water lines if the water is in the cell, and turning off the field could shift one of these lines far enough to make it seem to disappear. In addition, turning off the field sometimes causes a shift in the pen position. These uncertainties make this test not quite reliable.

The most reliable way to test a suspect line is to observe the line several times as the field is decreased toward zero. This gradual decreasing of the field allows the observer to keep up with any changes in energy, and if the line is a hydrogen line the absorption will

decrease in a predictable manner as the field is decreased. The $Q_1(0)$, $Q_1(1)$, $Q_1(2)$ and $Q_1(3)$ hydrogen fundamental lines are shown in Figure 13. The effects of decreasing the field is shown in Figure 14 for the $Q_1(1)$ fundamental line.

The pure rotational lines were run using the carbon rod furnace as an infrared source, the 30 groove per m.m. grating, a sodium chloride or potassium bromide prism and the liquid helium cooled copper-doped germanium detector. Again all of these components have been discussed in the previous sections.

The running conditions for the $S_o(1)$ line shown in Figure 15 were close to ideal. The line was run in the third order of the grating and was calibrated using the R(0) and R(3) CO lines in the eleventh order of the grating. The potassium bromide prism was used to separate the orders of the grating. A linear interpolation was used to determine the position of the hydrogen line.

The conditions for the $S_o(2)$ and $S_o(3)$ hydrogen lines shown in Figure 16 were not nearly so ideal. The $S_o(2)$ in the fourth order of the grating and the $S_o(3)$ in the fifth order lay very close together on the grating so it was decided to run the lines at the same time. The lines were between the tenth and eleventh orders of CO on the grating, and both orders were used for calibration. Due to the overlapping order of the CO lines, not all the lines were usable. However, at least eleven lines were usable in each run. The usable lines were considered to be too far away from the unknown lines for

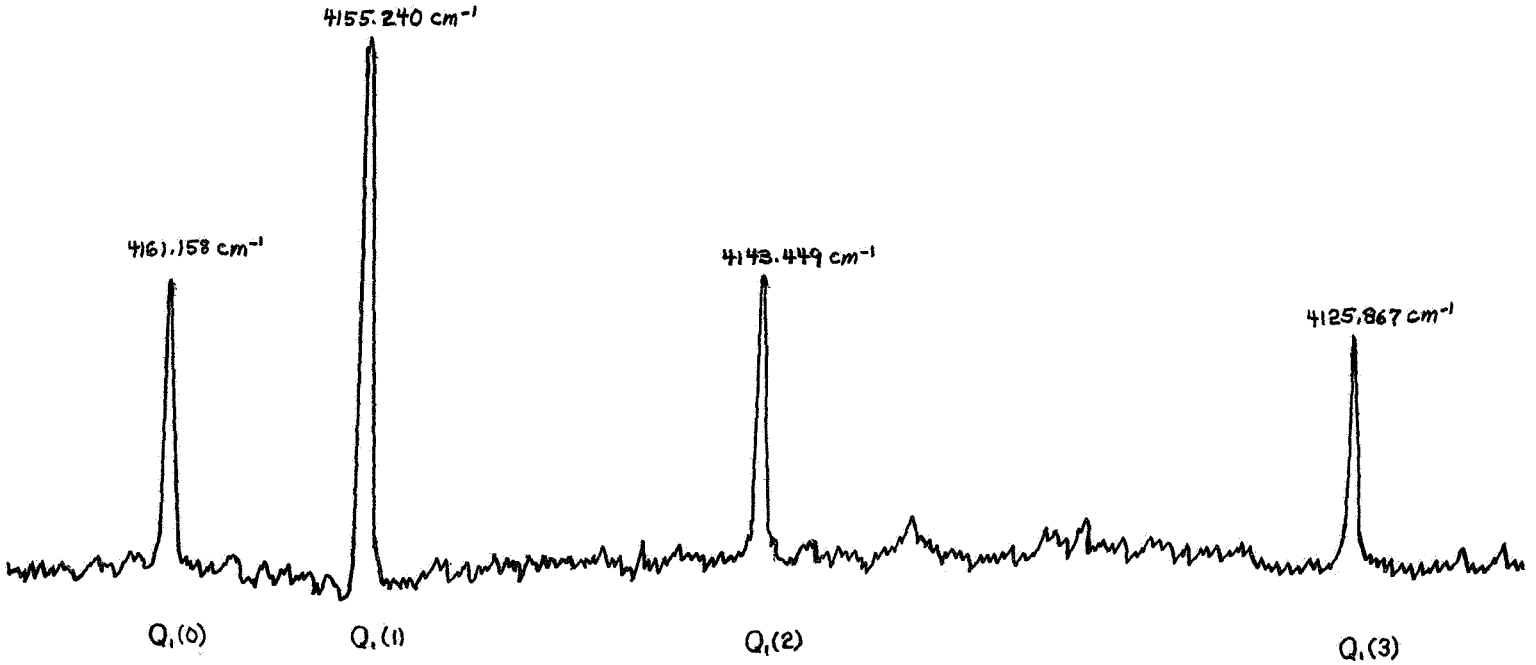

Figure 13. A portion of the hydrogen fundamental spectum

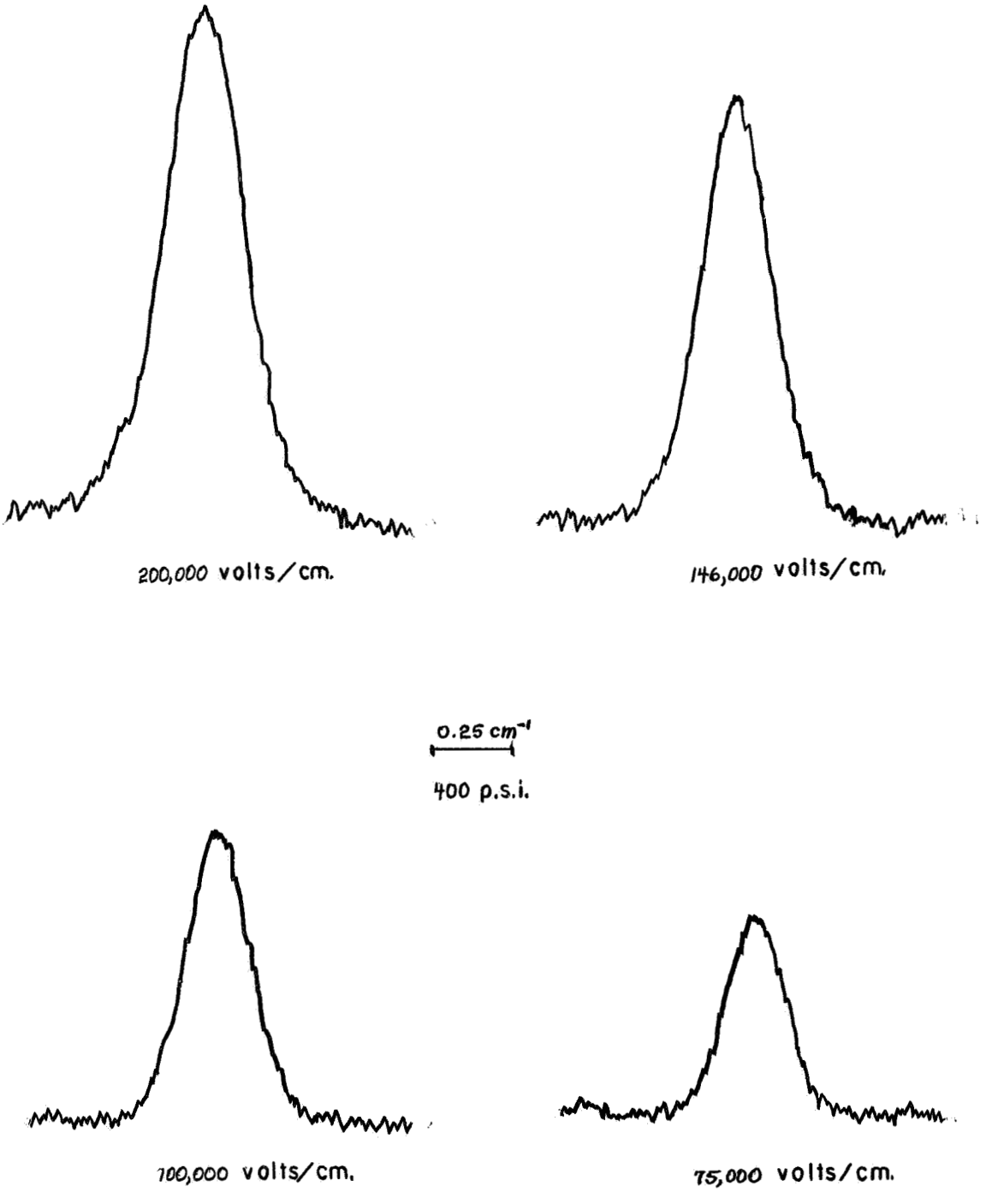

Figure 14. Field dependence of the $Q_1(1)$ line

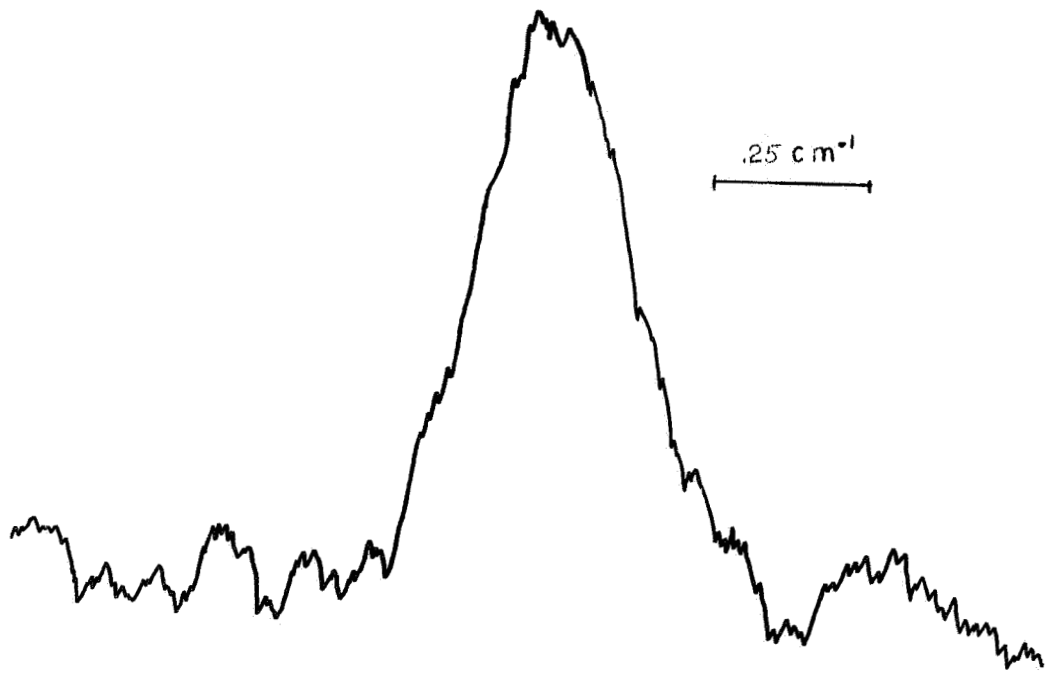

Figure 15. $S_0(1)$ pure rotational hydrogen line

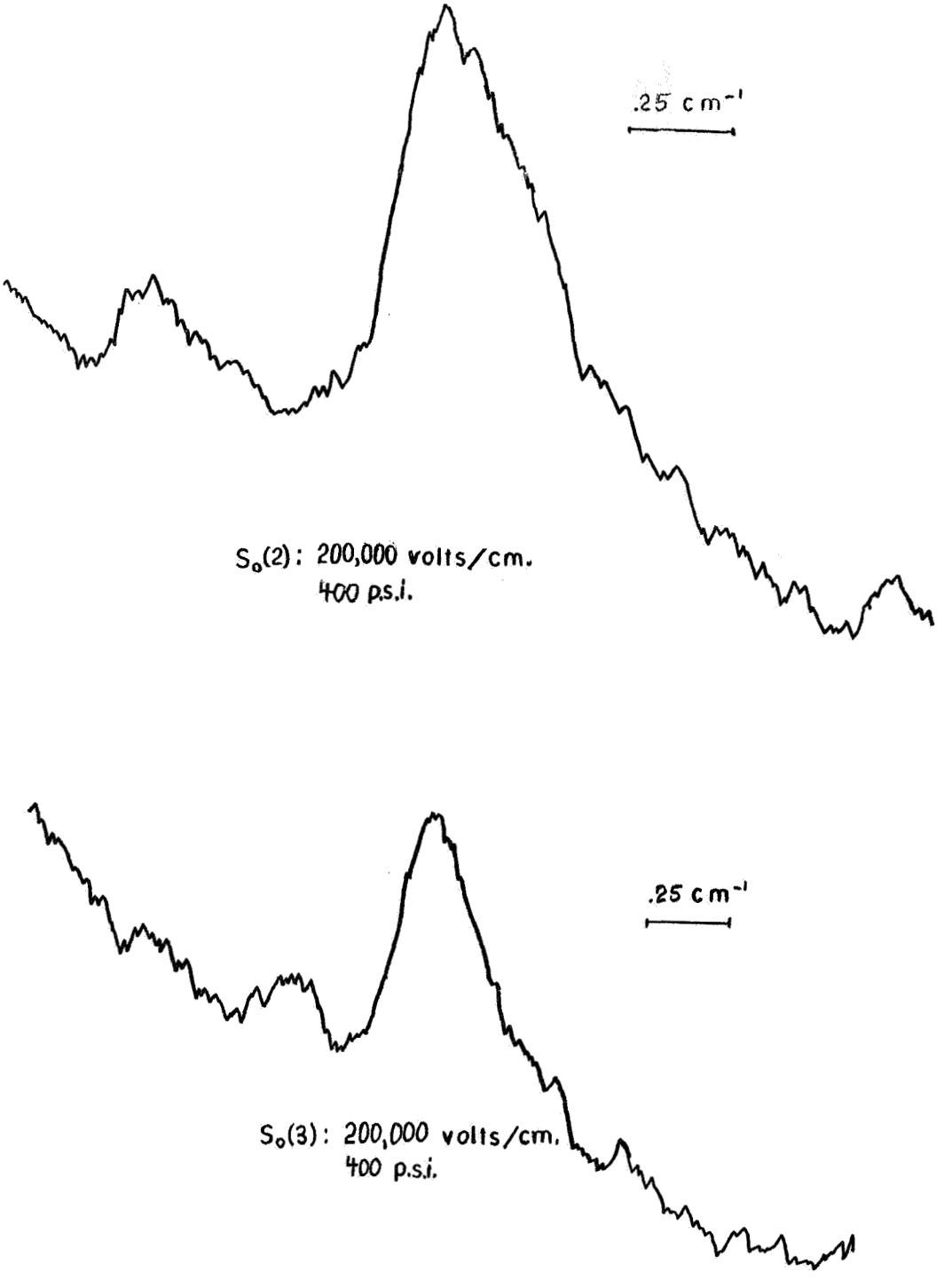

Figure 16. $S_0(2)$ and $S_0(3)$ pure rotational hydrogen lines

a linear interpolation. Therefore the unknown line positions were determined by using a curve determined from the best fit of the CO lines to the equation:

$$\nu = A_1 + B_1 X + C_i X^2 + D_1 X^3$$

where ν is the frequency of the line and X is its chart position measured from some arbitrary starting point. A computer program was used to determine the coefficients of this equation using the known CO frequencies and chart positions, and then used the curve of best fit to determine the frequencies of the hydrogen lines from their chart positions.

The line centers of the CO calibration lines and the $S_o(1)$ hydrogen line were determined by drawing a number of lines parallel to the base line.

The line center was taken to be the average of the centers of these parallel lines. The $S_o(2)$ and $S_o(3)$ lines were on sloped base lines which made line center determinations more difficult, since the angle of the base line was not constant over a long enough length. The sloped base was an instrumental difficulty and was due to the energy curve coming from the prism. The change in energy in the vicinity of the lines was very rapid, and with the reproducibility and course adjustment of the prism, it was impossible to put these lines at the bottom of the curve where the base was almost flat.

At first the sloped base was considered to be a serious problem and would shift the measured line center by a considerable amount. However the angle of the base line was not nearly so great as it appeared. These two lines were run with an off-set signal fed into the amplifier so that the 100% absorption level was far beyond the top of the recording paper. The high gain magnified the slope and made it appear to be as much as 30^{o}. The change in energy, however, from one side of the line to the other was in no case greater than 4% and was in most cases only about 2%. This is close to a flat base line and its effect on the position of the line center should be less than the accuracy of the line center measurements. Attempts to correct for the effects of the sloped base by, point by point subtraction merely confirmed the fact that the base was almost flat, since the subtraction process made the lines increasingly asymmetric as the angle of the base was increased. The line centers were measured, therefore, by drawing a number of lines parallel to the edge of the paper through the unknown line and finding the average of the centers of these lines.

An additional correction had to be made for the $S_o(2)$ line to find its line center. A weakly absorbing atmospheric line (probably H_2O) lay under the high frequency side of this line, and its effect was enough to make the line asymmetric so that its line center would be difficult to measure. The $S_o(1)$ and $S_o(3)$ hydrogen lines were observed to be symmetric within the limits of the noise, and

so the $S_o(2)$ line was assumed to be symmetric when the effect of the atmospheric line was neglected. The line was superimposed on the high frequency side of the line and did not seem to affect the shape of the low frequency side. This low frequency side was therefore traced on paper and then reversed and transferred to the other side of the line. The line centers were then determined in the manner described above.

The pure rotation lines were calibrated exclusively with CO absorption lines. The frequencies of these lines in the proper order were taken from Rao (19). Since the lines were run in air, these vacuum frequencies were converted to air values using the tables by Edlén reproduced in Rao (19). The measured frequencies of the pure rotation lines were therefore in air values and were converted back to vacuum frequencies, again using Edlén's tables in Rao (19).

CHAPTER V

RESULTS

The measured line frequencies of the pure rotation lines of hydrogen are shown in Table V and are compared to the frequencies measured by Stoicheff (5) using Raman techniques and the frequencies calculated by Brannon (10) from constants obtained from electric field induced work with the fundamental vibration-rotation lines of hydrogen. The frequency of each line is higher than the values of either Stoicheff or Brannon. The position of the $S_o(1)$ line is only slightly higher and is very close to Stoicheff's data. However, the position of the $S_o(2)$ and the $S_o(3)$ lines is shifted upward by about 0.12 cm^{-1} from Stoicheff's data. These two lines were measured together and the possibility of a systematic error exists. The possible source of a systematic error of this magnitude is not known. The possible sources of error are:

1. Pressure shifts of the pure rotation lines of a magnitude greater than that predicted from the data of May, et.al.(11).
2. Pressure shift of the CO calibration lines due to the relatively high pressures (about one-half atmosphere) used in the calibration cell. This was necessary because of the short path length cell used and also due to the fact that the calibration lines used were near the end of the CO branch.

TABLE V

FREQUENCIES OF THE PURE ROTATION LINES

Line	Observed this Experiment (cm^{-1})		Observed by Stoicheff (cm^{-1})	Calculated by Brannon (cm^{-1})
$S_o(1)$	587.079	± .02	587.055	587.023
$S_o(2)$	814.523	± .05	814.406	814.400
$S_o(3)$	1034.765	± .05	1034.651	1034.622

3. The sloped base lines on which the two hydrogen lines were located.

4. The presence of the small atmospheric line under the $S_o(2)$ line.

The magnitude of the pressure shift of the hydrogen lines was considered negligible being of the order of magnitude of .01 cm^{-1}. The magnitude of the shift of the CO lines is very small and is negligible particularly in view of the fact that any shift is reduced by a factor obtained from the ratio of the order of the unknown line to the order of the CO lines. For example, in the case of the $S_o(2)$ line the factor would be 4/10. The effect of the base line has been discussed and was not great enough to produce a shift of this magnitude. The effect of the atmospheric line underneath the $S_o(2)$ line was corrected for approximately as discussed in the previous chapter and could not in any case have produced such a large shift. In light of the close agreement of the molecular constants with the data of Stoicheff (5) and Brannon (10) even with the limited amount of data used to determine the constants, it is felt that the relative positions of the lines are correct. Further work with the elimination of the possible sources of error mentioned should determine the positions of the lines more accurately.

The molecular constants calculated from the appropriate equations from Table I on page 9 are given in Table VI. These are compared to those calculated by Stoicheff (5) and Brannon (10) and agree favorably with both. The value of H_o does not agree as well but is satisfactory considering the limited amount of data used to determine the constants.

TABLE VI

MOLECULAR CONSTANTS OF HYDROGEN

Calculated this Experiment(cm^{-1})		Calculated by Stoicheff(cm^{-1})		Calculated by Brannon(cm^{-1})	
59.332	± .005	59.339	± .005	59.334	± .003
.0450	± .004	.0443	± .003	.0457	± .0003
3.1×10^{-5}	± 1×10^{-5}	5.2×10^{-5}	± 5×10^{-6}	4.5×10^{-5}	± 8×10^{-6}

CHAPTER VI

CONCLUSION AND SUGGESTIONS FOR FUTURE WORK

In conclusion the electric field induced technique for observing normally forbidden infrared transitions is a valuable tool for probing the structure of homonuclear molecules. Second generation Stark cells with no spacers between the plates should provide higher electric field intensities and enable more lines to be observed. Intensity and line shape measurements should become more accurate with the increased line intensities due to the higher fields. Probably the most important next step in the field of electric field induced spectrum is to look for the infrared spectrum of the nitrogen and oxygen molecules. A very high resolution spectrometer would be required for this work since the lines would be much closer together than the hydrogen lines.

Several molecules such as CO_2 have normally forbidden transitions which might be observed using the Stark effect to reduce the symmetry of these modes. It might also be possible to increase the magnitude of a small dipole moment in a molecule to enhance the observation of its infrared spectrum.

There are other more specialized studies to be done such as an extension of the work done in this experiment with the pure rotation lines:

1. Look for the $S_o(0)$ line and possibly the $S_o(4)$ line.
2. Determine the frequencies and molecular constants more accurately.

3. Study the pressure shifts of the lines.

4. Make intensity and line shape measurements.

In the fundamental vibration-rotation spectrum of hydrogen the lines are strong enough to make good subjects for a study of frequency shift due to the applied electric field.

The full utility of the electric field induced technique has not nearly been fully exploited and should provide an increasing wealth of knowledge of molecular processes in the future.

LIST OF REFERENCES

LIST OF REFERENCES

1. G. Hertzberg, in G. P. Kuiper's The Atmospheres of the Earth and Planets, Chicago, p. 346 (1949).

2. G. Hertzberg, Nature 163, 170 (1949).

3. D. H. Rank and T. A. Wiggens, J. Opt. Soc. of Am. 53, 759 (1963).

4. F. Rasetti, Physic. Rev. 34, 367 (1929).

5. B. P. Stoicheff, Can. J. Phys. 35, 730 (1957).

6. E. U. Condon, Phys. Rev. 41, 759 (1932).

7. M. F. Crawford and R. E. MacDonald, Can. J. Phys. 36, 1022 (1958).

8. R. W. Terhune and C. W. Peters, J. of Molecular Spect. 3, 138 (1959).

9. C. H. Church "High Resolution Electric Field Induced Infrared Absorption Spectra of H_2 and D_2" Thesis, U. of Michigan (1959).

10. P. J. Brannon "Pressure Effects on the Vibrational-Rotational Spectrum of H_2" Thesis, U. of Michigan (1964).

11. A. May, V. Degen, J. Stryland and H. Welsh, Can. J. Phys. 39, 1769 (1961).

12. J. L. Dunham, Phys. Rev. 76, 647 (1949).

13. M. F. Crawford and I. R. Dagg, Phys. Rev. 91, 1569 (1953).

14. V. Foltz, D. H. Rank and T. A. Wiggens, J. Mol. Spectroscopy 21, 203 (1966).

15. J. M. Meeks and J. D. Craggs, Electrical Breakdown of Gases, Oxford Press, pp. 297, 301, 327 (1953).

16. R. Spanbauer, P. E. Fraley and K. N. Rao, Applied Optics, 2 No. 12, 340, Dec. 1963.

17. T. A. Wiggens, U. of Penn., Personal Correspondence.

18. J. A. Herndon, W. E. Deeds, N. M. Gailar, W. F. Herget, R. J. Lovell, A. H. Nielsen, J. Opt. Soc. Am. 52, 1108 (1962).

19. K. Narahari Rao, C. J. Humphreys and D. H. Rank, Wavelength Standards in the Infared, Academic Press, New York, London (1966).

VITA

William Joseph Boyd, III was born in [redacted] on [redacted] He attended elementary schools in Newbern, North Carolina; Alcoa, Tennessee; and Dyersburg, Tennessee, and graduated from Dyerburg High school in 1961. He attended Southwestern at Memphis his freshman and sophmore years and transferred to The University of Tennessee at the beginning of his junior year. After two years at Knoxville and one summer at The University of Tennessee, Martin Branch, he received a Bachelor of Science degree in Physics from The University of Tennessee in June 1965. He entered graduate school at The University of Tennessee the following September and received his Master of Science degree in Physics in June, 1969. His experience in the field of optics has been supplemented by three summers' experience in the Fiber Surface Research section at E. I. DuPont de Nemours in Kinston, North Carolina.